



**HAL**  
open science

# Carbon fiber reinforced polymer metallization via a conductive silver nanowires polyurethane coating for electromagnetic shielding

David Dupenne, Antoine Lonjon, Eric Dantras, Thierry Pierré, Marc Lubineau, Colette Lacabanne

## ► To cite this version:

David Dupenne, Antoine Lonjon, Eric Dantras, Thierry Pierré, Marc Lubineau, et al.. Carbon fiber reinforced polymer metallization via a conductive silver nanowires polyurethane coating for electromagnetic shielding. *Journal of Applied Polymer Science*, 2020, pp.50146. 10.1002/app.50146 . hal-03033572

**HAL Id: hal-03033572**

**<https://hal.science/hal-03033572>**

Submitted on 1 Dec 2020

**HAL** is a multi-disciplinary open access archive for the deposit and dissemination of scientific research documents, whether they are published or not. The documents may come from teaching and research institutions in France or abroad, or from public or private research centers.

L'archive ouverte pluridisciplinaire **HAL**, est destinée au dépôt et à la diffusion de documents scientifiques de niveau recherche, publiés ou non, émanant des établissements d'enseignement et de recherche français ou étrangers, des laboratoires publics ou privés.



## Open Archive Toulouse Archive Ouverte





OATAO is an open access repository that collects the work of Toulouse researchers and makes it freely available over the web where possible

This is an author's version published in: <https://oatao.univ-toulouse.fr/26866>

### Official URL:


<https://doi.org/10.1002/app.50146>

### To cite this version:

Dupenne, David  and Lonjon, Antoine  and Dantras, Eric  and Pierré, Thierry and Lubineau, Marc and Lacabanne, Colette  *Carbon fiber reinforced polymer metallization via a conductive silver nanowires polyurethane coating for electromagnetic shielding.* (2020) Journal of Applied Polymer Science. 50146. ISSN 0021-8995.

Any correspondence concerning this service should be sent to the repository administrator: [tech-oatao@listes-diff.inp-toulouse.fr](mailto:tech-oatao@listes-diff.inp-toulouse.fr)

# Carbon fiber reinforced polymer metallization via a conductive silver nanowires polyurethane coating for electromagnetic shielding

David Dupenne<sup>1,2</sup> | Antoine Lonjon<sup>2</sup>  | Eric Dantras<sup>2</sup> | Thierry Pierré<sup>1,3</sup> | Marc Lubineau<sup>3</sup> | Colette Lacabanne<sup>2</sup>

<sup>1</sup>IRT A. de Saint Exupéry, Toulouse, France

<sup>2</sup>CNRS, UPS, Physique des Polymères, CIRIMAT, Université de Toulouse, Toulouse, France

<sup>3</sup>Thales Alenia Space, Toulouse, France

## Correspondence

Antoine Lonjon, CNRS, UPS, Physique des Polymères, CIRIMAT, Université de Toulouse, 118 route de Narbonne, Toulouse 31062, France.  
Email: antoine.lonjon@univ tlse3.fr

## Funding information

Agence Nationale de la Recherche; Commissariat Général aux Investissements

## Abstract

For electromagnetic shielding in space environment, the metallization of carbon fiber reinforced polymer (CFRP) is required. A specific attention is paid due to the thermal expansion coefficient difference between substrate and metal coating. A surface metallization of a CFRP has been elaborated by electrodeposition. This study presents an original process based on an electrically conductive polymer coating elaborated from a polyurethane matrix filled with a low content of silver nanowires (<10%vol). A continuous and adherent deposit is obtained by an optimization of the electroplating parameters. A minimal volume fraction was determined at 3%vol associated with an applied current density estimated near 0.1 A/dm<sup>2</sup>. The growth speed is 7 μm/h at 0.1 A/dm<sup>2</sup>. The adhesion was checked in severe environmental conditions (−196 to 165°C). The effectiveness shielding obtained with this solution reaches an attenuation value higher than 90 dB between 1 and 26 GHz necessary for space communication applications.

## KEYWORDS

coatings, composites, electromagnetic shielding, nanocrystals, nanoparticles, nanowires

## 1 | INTRODUCTION

The weight reduction in space transportation applications is a key point to limit the energy consumption. A large weight increase of the embedded electronic devices is due to the protection against the electromagnetic interferences (EMI). The EMI could affect the signal information generated or received by electronic equipment. The conventional solution consists in a shielding of the equipment by an impervious metallic box containing the electronic devices. In the case of satellites telecommunications systems, the weight of this metallic structure could be more important than the electronic equipment itself. The EMI encountered in satellites could emanate

from a wide variety of sources (equipment and devices)<sup>1</sup> and affect the electronic and electrical equipment performances. This kind of application must be protected with high shielding effectiveness in the gigahertz frequency range.<sup>2–8</sup> The best results for shielding are obtained with metals<sup>9</sup> due to their high electrical conductivity. The metal structure was realized in aluminum due to his low density: then, the surface is electroplated by a high electrical conductive metal like gold or silver.

The weight reduction of these metallic shielding structure can be achieved by replacing the metal components structure by carbon fiber reinforced polymer (CFRP), according to mechanical and mass properties requirements. The weight saving relative to the

mechanical performances is estimated near 30%.<sup>10</sup> In all cases the CFRP must be metallized to reach the shielding requirement. The CFRP surface conductivity is not enough to allow an electrodeposition classically used on aluminum. The application of a conductive underlayer is necessary to reach a highly conductive surface. This underlayer can be realized by different processes as electroless deposition,<sup>11</sup> chemical vapor deposition,<sup>12</sup> physical vapor deposition,<sup>13</sup> and dynamic chemical plating.<sup>14</sup> These processes create a metallic layer directly on the CFRP surface. But, this metal layer exhibits a weak surface adhesion. A dramatic detachment of this metal layer was observed for large temperature variation due to the difference of thermal expansion coefficient (CTE) with the CFRP substrate. This parameter is crucial for space applications due to the environmental temperature variation.

The conductive layer between the CFRP and the electroplated metal surface is the key point to permit an effective shielding on a wide temperature range. This layer must be sufficiently conductive to allow the electroplating, mechanically optimized to withstand the difference of thermal expansion coefficient and promoted a significant final grip of the metal surface layer. These specifications orientate our choice towards organic conductive layers. Intrinsic conductive polymers<sup>15–18</sup> could be used as conductive layer but their electrical conductivity are very dependent from temperature. Furthermore, their sensitivity to oxidation prevent them from an industrial application. A conductive composite coating polymer-based was preferred. Their extrinsic conductivity is time stable and along the electroplating process. The choice of the metallic filler to realize the conductive coating was essentially led by their electrical conductivity level and their resistance to oxidation. Metallic particles provide the highest electrical conductivity such as silver,<sup>19,20</sup> gold,<sup>21,22</sup> nickel,<sup>23</sup> and copper.<sup>20,24</sup> The conductive composites filled with silver particles are preferred to prevent the oxidation phenomenon. The percolation threshold is established around 15%vol<sup>25</sup> for spherical silver particles and the conductivity level is reached around  $10^2$  S/m.<sup>25,26</sup> Conventional conductive coatings are filled with 20%vol of silver particles. This filler content increases significantly the composite weight and deteriorates its mechanical properties. Lower percolation threshold could be obtained by increasing the particles aspect ratio  $\xi$  (ratio length to diameter).<sup>25,27</sup> Previous works of conductive composites filled with carbon fibers and Carbon NanoTubes (CNT) exhibit a low percolation threshold near 0.1–1%wt and an electrical conductivity around  $10^{-2}$ – $10^{-1}$  S/m above the percolation threshold.<sup>28–30</sup> Silver nanowires (AgNWs) with high aspect ratio allow us to provide a higher electrical conductivity for a small

amount of nanowires (below 5%vol). For these low rates,<sup>31</sup> the mechanical properties were preserved.

The aim of this study is to metallize CFRP substrate via a conductive underlayer composed of polyurethane (PU) matrix and AgNWs. We use a waterborne two-component PU to limit solvent emissions (volatile organic compounds) studied in a previous work.<sup>32</sup> The electrical conductivity behavior of the PU/AgNWs coating is presented. Above the percolation threshold, the conductivity level allows the metallic electroplating. The minimal volume fraction of AgNWs to obtain a continuous metallic deposit is studied. The adhesion of this deposit according to the applied current density is discussed. The conductive coating adhesion is analyzed as function of temperature. Finally, the shielding effectiveness for different configurations is measured and shows the interest to metallize CFRP.

## 2 | EXPERIMENTAL SECTION

### 2.1 | Nanowires processing

AgNWs were synthesized by reducing  $\text{AgNO}_3$  with ethylene glycol in presence of poly(vinyl pyrrolidone) ( $M_w = 55,000$  g/mol). The reaction was carried out at  $160^\circ\text{C}$  in a round-bottom balloon with magnetic stirring bar for 1 h. This technique and the solution concentrations were described by Sun et al.<sup>33,34</sup> AgNWs were elaborated in this work with only few variations.<sup>19</sup> This process permits to obtain nanowires with an aspect ratio around 222.<sup>19</sup> After the process, AgNWs were cleaned by successive washing of water and ethanol. Clean AgNWs were stored in ethanol and dispersed using an ultrasonic bath for short time.

### 2.2 | Electrodeposition processing

Silver electroplating of CFRP process was achieved in two steps: First, the coating application of PU/AgNWs on CFRP to obtain a conductive surface layer followed by the silver electroplating. For this last step, an original silver electroplating cyanide free bath based was used.

- Step 1: PU/AgNWs coating on CFRP: The PU coating is a two components system: Poly(2-hydroxypropylmethacrylate) (PHPMA), MACRYNAL<sup>®</sup> VSM 6299w/42WA (Allnex, Belgium), in 40%wt water; and Easaqua<sup>™</sup> X D 401 (Vencorex, France) composed of hexamethylene diisocyanate, isocyanurate (45%wt), and 3-isocyanatomethyl-3,5,5-trimethylcyclohexyl isocyanate (30%wt) in 15%wt *n*-butyl acetate. The two

parts are mixed at room temperature (ratio 3:1) with the appropriate volume fraction of AgNWs. The mixture is sprayed with a high volume low pressure (HVLP) spray gun. The curing process is 30 min at 80°C.

- b. Step 2: Silver electroplating of PU/AgNWs: The electrolysis was performed at 50°C with silver as anode and the PU/AgNWs coating on CFRP as cathode. The composition of silver electroplating bath is gathered in Table 1. The metallic coating adhesion depends on the current density. The current density value will be discussed in this work.

### 2.3 | Scanning electron microscopy

The coating surface was observed using a JEOL JSM 6700F. Images were collected under 10 keV accelerating voltage and were obtained using the back-scattered electron detection mode.

### 2.4 | Electrical conductivity

The electrical conductivity of the PU/AgNWs composites was measured by a four-point probe technique using a Keithley 2420 for sample impedance less than 10 Ω. The electrical conductivity measurements were carried out by recording the complex conductivity  $\sigma^*(\omega)$  using a Novocontrol broadband spectrometer (BDS) for impedance above 10 Ω. Measurements were done in the frequency range from  $10^{-2}$  to  $10^6$  Hz at room temperature. The real part,  $\sigma'(\omega)$  of the complex conductivity  $\sigma^*(\omega)$  was investigated. The value of  $\sigma'(\omega)$  at  $10^{-2}$  Hz was taken as DC conductivity  $\sigma_{dc}$ .

The bulk electrical conductivity is determined from the measured resistance of the sample between two electrodes. Samples were disks with a diameter of 20 mm and

**TABLE 1** Composition of silver electrodeposition cyanide free bath

Chemical component	Chemical formula	Mass concentration (g/L)
Silver methanesulfonate	CH <sub>3</sub> AgO <sub>3</sub> S	10.15
Boric acid	H <sub>3</sub> BO <sub>3</sub>	10
Sodium sulfite	NaSO <sub>3</sub>	13.2
Sodium thiosulfate	Na <sub>2</sub> S <sub>2</sub> O <sub>3</sub>	52.1

thickness of 500 μm. Samples were placed between 20 mm gold plated electrodes.

The surface electrical conductivity  $\sigma_{surf}$  is related to the measured resistance  $R_{surf}$  according to ASTM D257 between two concentric electrodes separated by an insulator at the surface of the sample:

$$\sigma_{surf} = \frac{\ln \frac{R_2}{R_1}}{2\pi R_{surf}} \quad (1)$$

With  $R_1$  and  $R_2$  the radius of the inner and outer electrode, respectively. Samples were coating (thickness ~ 50 μm) on isolated substrates of  $12 \times 12$  cm<sup>2</sup>. The conductivity is normalized to surface unit (S.Sqr).

### 2.5 | Adhesion test

The adhesion strength of the plated silver deposit was estimated by a cross-cut tape test (ISO 2409). This test consists in applying and removing a pressure-sensitive adhesive tape over 25 cross-hatched squares of  $2 \times 2$  mm<sup>2</sup>. The cut area of the test coating was examined and classified from 0 (excellent adhesion) to 5 (bad adhesion) by a visual comparison with illustrations in the standard, depending on the amount of flaked coating.

### 2.6 | Thermal expansion and complex mechanical compliance

The thermal expansion coefficient  $\alpha$  and the complex mechanical compliance  $J_{\omega}^*(T)$  was determined by dynamic mechanical analysis using an ARES G1 strain controlled rheometer (Rheometrics Scientific). Experiments were carried out in rectangular torsion geometry over the linear range ( $10^{-2}\%$  strain at angular frequency of 1 rad/s) from -145 to 150°C with an heating rate of 3°C/min. PU and composites samples were sprayed on silicone mold with 45 mm in length and 10 mm in width. After the curing process, the sample thickness is approximately 500 μm.

### 2.7 | Electromagnetic shielding

The electromagnetic shielding was carried out with a mode-stirred reverberation chamber SMART 700 Chamber (ETS-Lindgren). The frequency range was from 1 to 26 GHz. The samples dimensions were

$12 \times 12 \text{ cm}^2$  screwed on an aluminum casing with a silicone seal filled with silvered copper particles. The treated surface (conductive coating or metallic deposit) has been oriented inwards to maximize electrical continuity. The effectiveness criterion over the frequency range tested is chosen at 90 dB (dependent on application). Before each test, the shielding effectiveness of a  $50 \Omega$  standard is measured to check the coaxial cable state linked to aluminum casing. The effectiveness measured is the maximal effectiveness accessible by the mode-stirred reverberation chamber.

### 3 | RESULTS AND DISCUSSIONS

#### 3.1 | Conductive PU/AgNWs coating

The bulk and surface conductivity of the PU/AgNWs coating were measured as function of AgNWs volume fraction and given in Table 2. At low volume fraction, the conductivity is close to the neat PU value, that is,  $10^{-14} \text{ S/m}$  for bulk and  $10^{-13} \text{ S.Sqr}$  for surface. The percolation threshold has been determined near 0.6%vol for bulk and 0.8%vol for surface. Above the percolation threshold, electrical conductivity values, 100 S/m for bulk and  $10^{-2} \text{ S.Sqr}$  for surface, are enough for electrodeposition process.

**TABLE 2** Bulk and surface conductivities of PU/AgNWs

Volume fraction (%)	Bulk conductivity (S/m)	Surface conductivity (S.Sqr)
0	$5 \times 10^{-14} \pm 4 \times 10^{-15}$	$1 \times 10^{-13} \pm 5 \times 10^{-14}$
0.2	$8 \times 10^{-14} \pm 1 \times 10^{-14}$	
0.5	$1 \times 10^{-13} \pm 3 \times 10^{-14}$	$5 \times 10^{-13} \pm 2 \times 10^{-13}$
0.7	$1 \times 10^{-2} \pm 3 \times 10^{-3}$	
1	$2 \times 10^{-1} \pm 1 \times 10^{-2}$	$3 \times 10^{-5} \pm 1 \times 10^{-6}$
1.5	$5.2 \pm 4 \times 10^{-1}$	
2	$10 \pm 2$	$2 \times 10^{-3} \pm 3 \times 10^{-4}$
3	$33 \pm 11$	$1 \times 10^{-2} \pm 4 \times 10^{-3}$
4	$68 \pm 23$	$3 \times 10^{-2} \pm 7 \times 10^{-3}$
5	$125 \pm 44$	$7 \times 10^{-2} \pm 6 \times 10^{-3}$
6	$120 \pm 32$	$9 \times 10^{-2} \pm 3 \times 10^{-3}$

Abbreviations: AgNWs, silver nanowires; PU, polyurethane.

### 3.2 | Electrolytic deposit

#### 3.2.1 | Electrodeposition lower limit

At low volume fraction of AgNWs in PU matrix, the electrodeposition process is possible. A continuous metallic deposit is obtained since a regular surface conductive network is formed at the microscopic scale. The gap between nanowires is an important parameter directly linked to the quantity of nanowires dispersed in the matrix.

The electrolytic deposits have been realized on coatings as function of AgNWs volume fraction with a current density of  $0.1 \text{ A/dm}^2$  during 2 h. The scanning electron microscopy (SEM) images are shown in Figure 1. No silver deposit was observed for a volume fraction of 0.7%vol close to the percolation threshold. Some metallic silver germs began to grow at 1%vol of AgNWs. The germs density increased with the volume fraction of nanowires and coalesced to form little clusters from 2.5%vol. The surface was totally covered by the silver deposit above 3%vol. This value is the lower limit to obtain a continuous silver layer on the conductive coating surface. The same result was confirmed for higher content of AgNWs. The optimal rate of nanowires was chosen at 4%vol to insure a good reproducibility of electrolytic deposit.

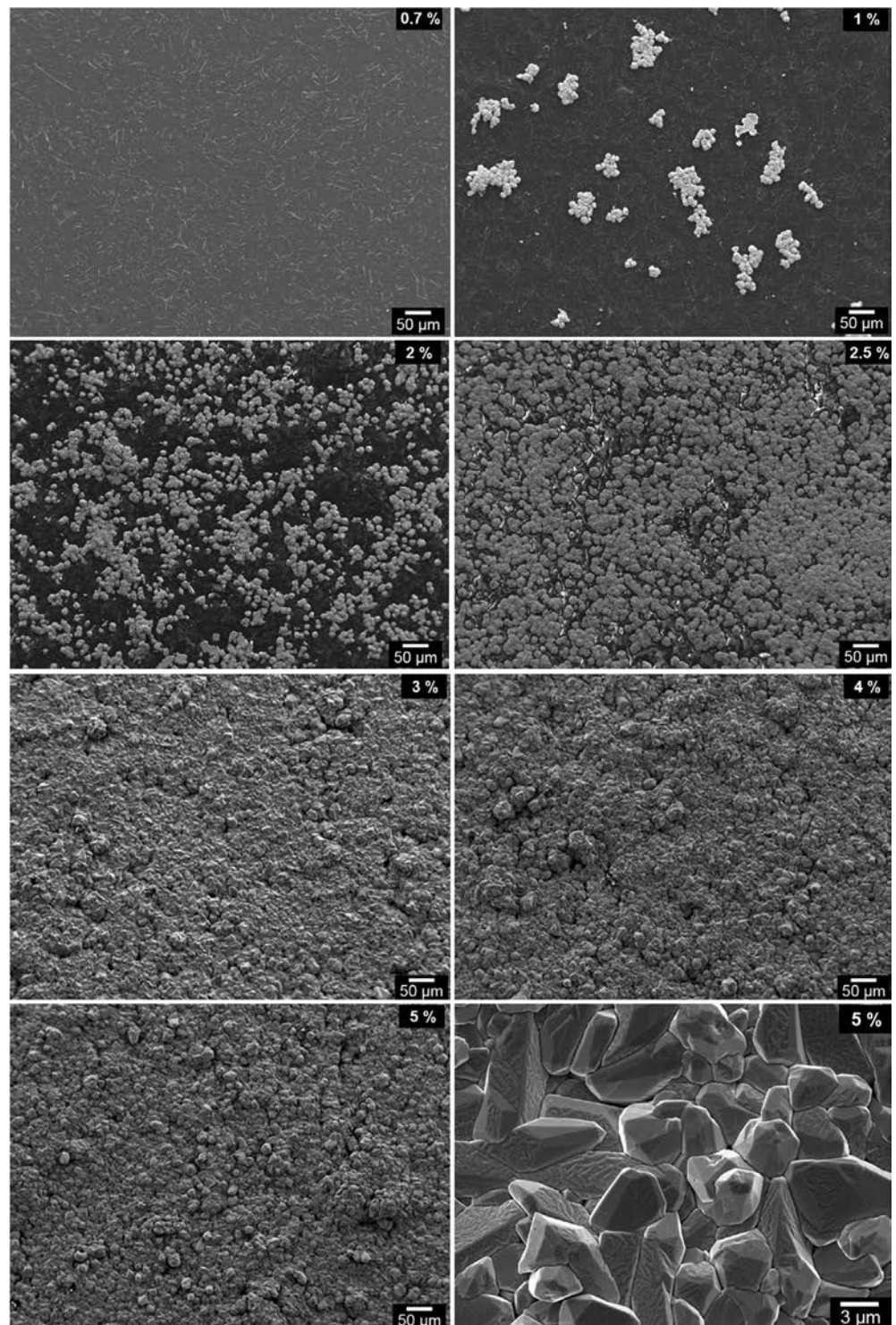
For the same rate of AgNWs, the current density influences the metallic deposit speed but also its microstructure. The germination phenomenon was improved by high current density inducing a silver layer growth in all directions. This uncontrolled growth provides a spongy silver structure. For low density, the germination becomes less important promoting the crystal growth as large crystal structures (Figure 2).

#### 3.2.2 | Apparent current density

The metallic deposit adhesion has been checked as function of the current density. The CFRP substrates have been coated with a layer of PU/AgNWs filled with 4% vol. The electrodeposition times have been adjusted to obtain metallic deposits with a quasiconstant thickness (between 10 and  $20 \mu\text{m}$ ). The adhesion quality, according to ISO 2409 standard, is represented versus the current density on Figure 2. For current densities lower than  $0.2 \text{ A/dm}^2$ , the adhesion class is 0 corresponding to a maximum adhesion. For higher current densities, the deposit adhesion is altered. This phenomenon is accentuated by the current density increase. In addition, we have observed a polymer surface degradation certainly due to a local increase of the temperature at the vicinity of



**FIGURE 1** Electrolytic deposits realized on coatings as function of silver nanowires volume fraction observed by scanning electron microscopy



metallic germs for high current density. This thermal degradation implies a decrease of the adhesion.

We observe a lack of adhesion of metallic deposit for high current density. In order to understand, the current density really seen by the AgNWs was studied. The current density  $J$  is dependent from the applied current  $A$  and the conductive surface  $S$ . The current lines are focused on the conductive fillers; that is, the conductive

coating is composed of an insulated polymer matrix and conductive nanowires. The electrolytic deposit is only initiated on the site occupied by AgNWs at the surface of the coating ( $S_{Ag}$ ).

The involved surface  $S_{Ag}$  has been determined by coupling the SEM images analysis of the PU/AgNWs coating surface with the nanowires volume fraction. This surface  $S_{Ag}$  corresponds to AgNWs area in direct contact with

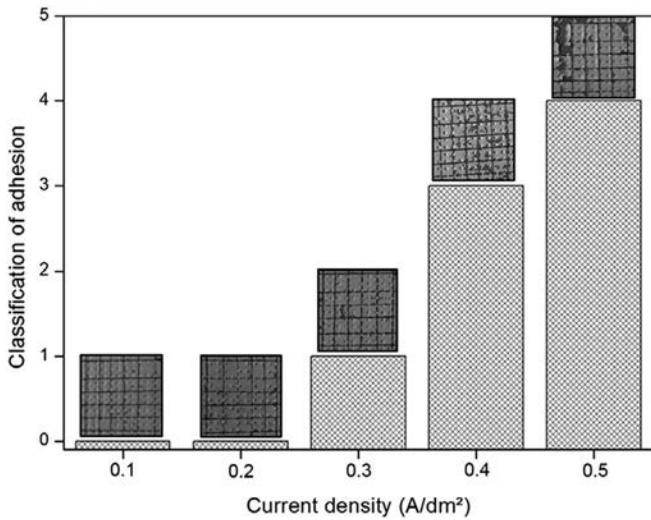


**FIGURE 2** Adhesion of electrolytic coating according to current density values

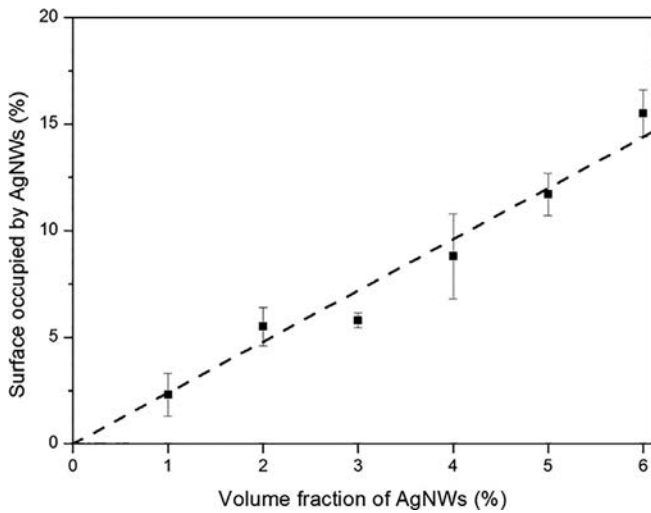


**FIGURE 3** Surface occupied by silver nanowires (AgNWs) versus the nanowires volume fraction

the electroplating bath and involve in the electrodeposition process. Data are reported in Figure 3. The behavior law is linear for coatings filled up to 6%vol. The electroactive AgNWs occupied surface is less than 20% for low volume fractions.

Figure 4 shows the apparent current density versus the AgNWs volume fraction for different applied current densities. The apparent current density corresponds to the current density normalized by  $S_{Ag}$ , determined by SEM observations of coating surface.

The applied current densities in electroplating on metal, as aluminum, are 0.5–1 A/dm<sup>2</sup>. For a 4%vol coating filled, we determined an apparent current density near 10 A/dm<sup>2</sup>. This high value induces an increase of

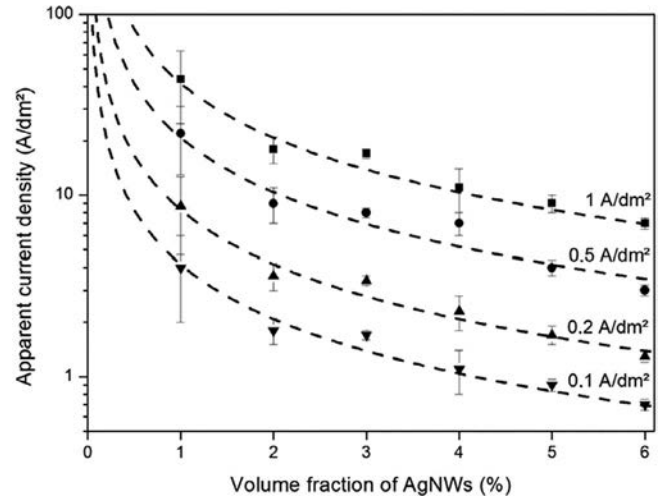


**FIGURE 4** Apparent current density of the polyurethane/silver nanowires (AgNWs) for different current density

local temperature at the AgNWs/PU matrix interface leading to polymer degradation. After the adhesion test, nanowires present on the surface are removed from the PU matrix and stay with the electrolytic deposit. The polymer degradation induced by high current density probably damage also the interactions between nanowires and polymer matrix.

If we applied a maximum value of current densities close to 0.2 A/dm<sup>2</sup> for a coating filled with 4%vol of AgNWs, the apparent current densities have similar values (or lower) than current densities values used classically for bulk metal surface. The interface between nanowires and polymer was preserved and a good value for adhesion test is obtained. In this work, we have chosen to process electrolytic deposits with a current density of 0.1 A/dm<sup>2</sup>. This last value allows us to obtain good reproducibility in term of the electrolytic deposit adhesion (Figure 5).

### 3.2.3 | Metallic deposit thickness

Parameters leading the deposit thickness are the current density value and the time. The deposit thickness has been studied for AgNWs content above the electrodeposition limit (from 3 to 6%vol) with a current density of 0.1 A/dm<sup>2</sup> during 2 h (Figure 5(a)). The thickness looks to be independent from the volume fraction. The homogeneous conductive network coated on the surface allows us to cover it with a continuous metal layer.

The Figure 5(b) describes the growth kinetics of the electrolytic deposit on the PU/AgNWs coating filled with 4%vol with a current density of 0.1 A/dm<sup>2</sup>. The growth is linear with a deposit speed around 7 μm/h. Literature



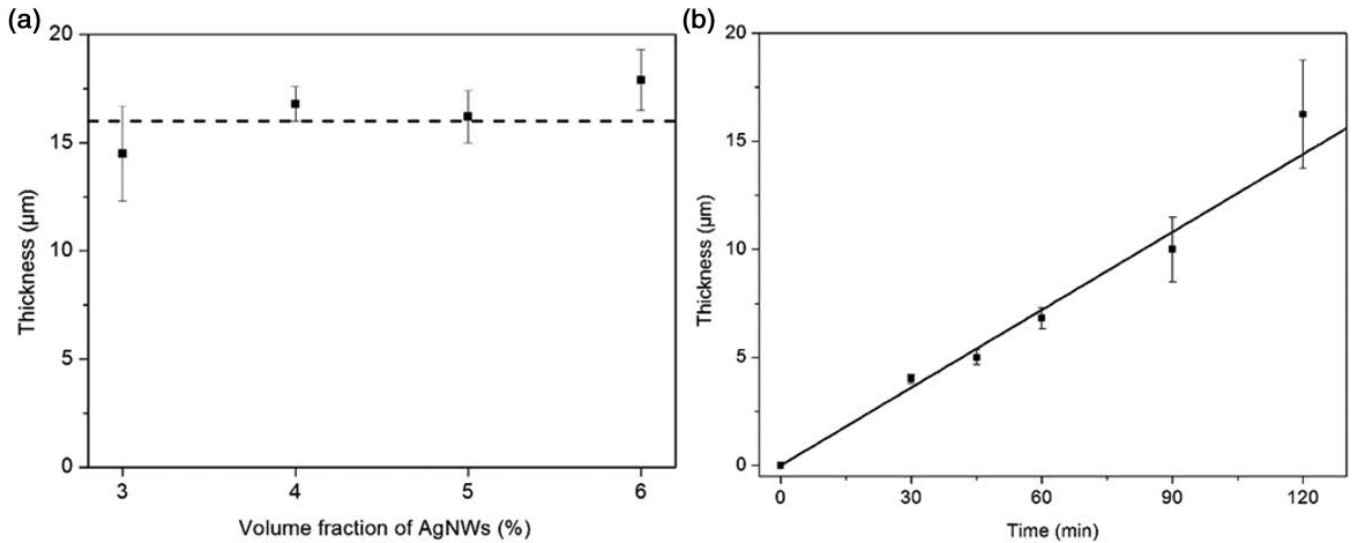


FIGURE 5 Electrolytic deposition thickness versus volume fraction of silver nanowires (AgNWs) (a) and time (b)

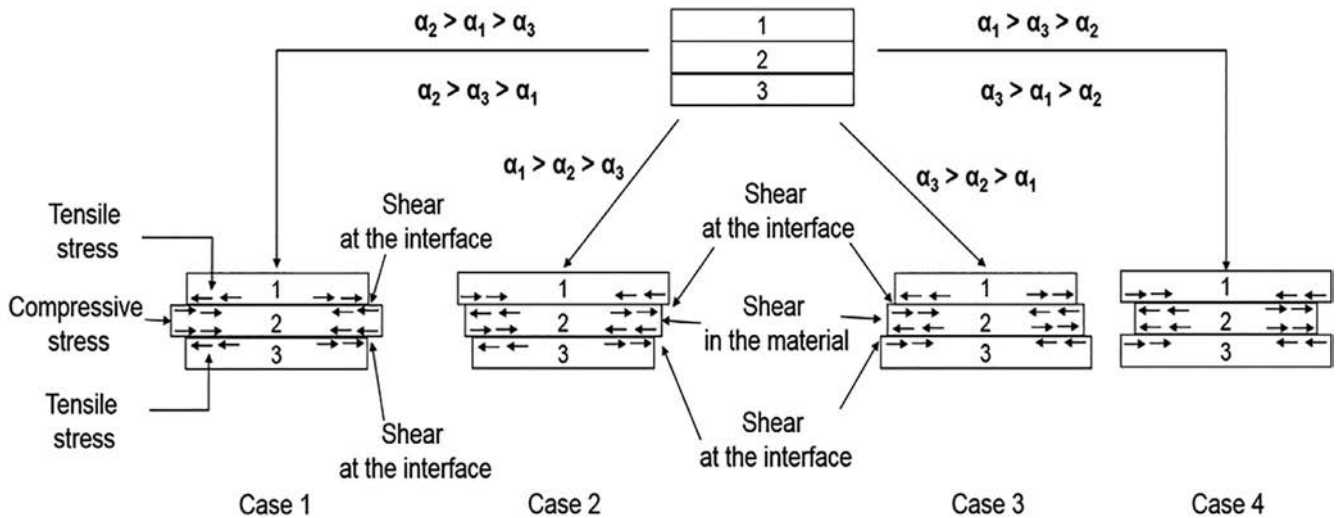


FIGURE 6 Schematic representation of stresses induced by the different coatings thermal expansion coefficients

reports an optimized electromagnetic shielding value for an electroplating thickness between 5 and 10 μm.<sup>35</sup> In this case, it is possible to obtain a shielding higher than 90 dB for the high frequencies domain close to 1 GHz. The Figure 5(b) allows us to extrapolate the corresponding electrolytic treatment time near 45 min to obtain the expected thickness.

### 3.3 | Adaptation of thermal expansion

Due to the space environment, the coatings adhesion is required on a wide temperature range (between -180 and 165°C). The thermal expansion coefficient (CTE) of CFRP is very different from the metallic layer. The CTE

difference would create mechanical stresses at the interface. The metallic layer adhesion could be altered during temperature cycling. So, weakly filled polymer coating between metallic layer and CFRP substrate could absorb the expansion difference.

In order to check these assumptions, different cases of stress versus CTE for a three layers assembly are shown in Figure 6. The first layer can be assimilated to the metallic deposit, the second layer to PU/AgNWs coating and the third layer to CFRP substrate. In the case 1 and 4, when the expansion coefficient of the conductive coating is higher or lower than two others layers (CFRP and metal), tensile and compressive stresses are opposite to interfaces, creating shear stresses. The PU/AgNWs coating presents a good

compatibility with the CFRP substrate, which allows to maintain adhesion with the presence of these stresses at interface. In the case 2 and 3, the expansion coefficient is intermediate which generates supplementary shear stresses in the PU/AgNWs coating. The conductive coating should have an expansion coefficient higher or lower than two others layers to limit shear stresses.

Strain versus temperature is shown for the CFRP substrate, the PU matrix, the PU/AgNWs coating filled with 2%–6%vol and bulk silver on the Figure 7(a). The thermal expansion coefficients are given in Table 3.

For silver bulk and CFRP substrate the strain behavior as function of temperature is quasi linear. For PU matrix and PU/AgNWs composites, the thermal expansion coefficient is dependent on  $T_g$ . Two coefficients  $\alpha$  are observed according to vitreous and rubbery states.  $\alpha$  value is not dependent on nanowires ratio in the vitreous state; it is due to the weak mobility below  $T_g$ . In contrast,  $\alpha$  values increases above  $T_g$  and decrease with nanowires content. Nanowires play the role of additional entanglements for macromolecules on the rubbery plateau. Despite these modification, PU/AgNWs composites point out an  $\alpha$  value higher than silver bulk and CFRP substrate. This configuration is consistent with the case 1 of Figure 6.

The adaptation of thermal expansion phenomenon could be described by the thermal expansion coefficient and mechanical compliance. The PU/AgNWs coating should have a high mechanical compliance to adapt the shear stresses at the interfaces. The storage compliance  $J'$  versus temperature is shown in Figure 7(b), calculated from storage  $G'$  and dissipative  $G''$  shear modulus as following:

$$J' = \frac{G'}{G'^2 + G''^2} \quad (2)$$

We note a storage compliance of the PU matrix higher than the silver and the substrate mechanical compliance over all the temperature range. At low temperature, the value is around  $10^{-9} \text{ Pa}^{-1}$  and reaches  $10^{-6} \text{ Pa}^{-1}$  for high temperature. The mechanical compliance decreases by insertion of AgNWs. For low volume fraction of AgNWs, the PU/AgNWs coating absorbs stresses by adapting the induced strain with the thermal expansion of different materials (case 1, Figure 6).

The thermal shocks cycling process was chosen to simulate the worst case for expansion adaptation. The estimated time between two extreme values of temperature is about 1 min. The maximal temperatures chosen are similar with the thermal cycling temperature ( $-180$  to  $165^\circ\text{C}$ ) in space environment. The system suffered two successive thermal shocks (cooling and heating) with temperature variation of  $360^\circ\text{C}$ . Figure 8 reports the schematic representation of the thermal cycling.

After two thermal shocks, adhesion test was performed to confirm the expansion adaptation of the CFRP metallized sample with the PU filled with 4%vol of AgNWs. An excellent adhesion value was obtained before the thermal treatment for a metallic deposit with a current density of  $0.1 \text{ A/dm}^2$ . After these two accelerated aging, a class 1 adhesion result was measured corresponding to the industry requirements. The PU matrix adapts the difference of thermal expansion coefficient of the CFRP substrate and the silver deposit absorbs the induced mechanical stresses. The higher compliance with a maintain of ductility is obtained with a volume fraction of AgNWs lower than 5%vol<sup>31</sup> and provides the expected adhesion level.

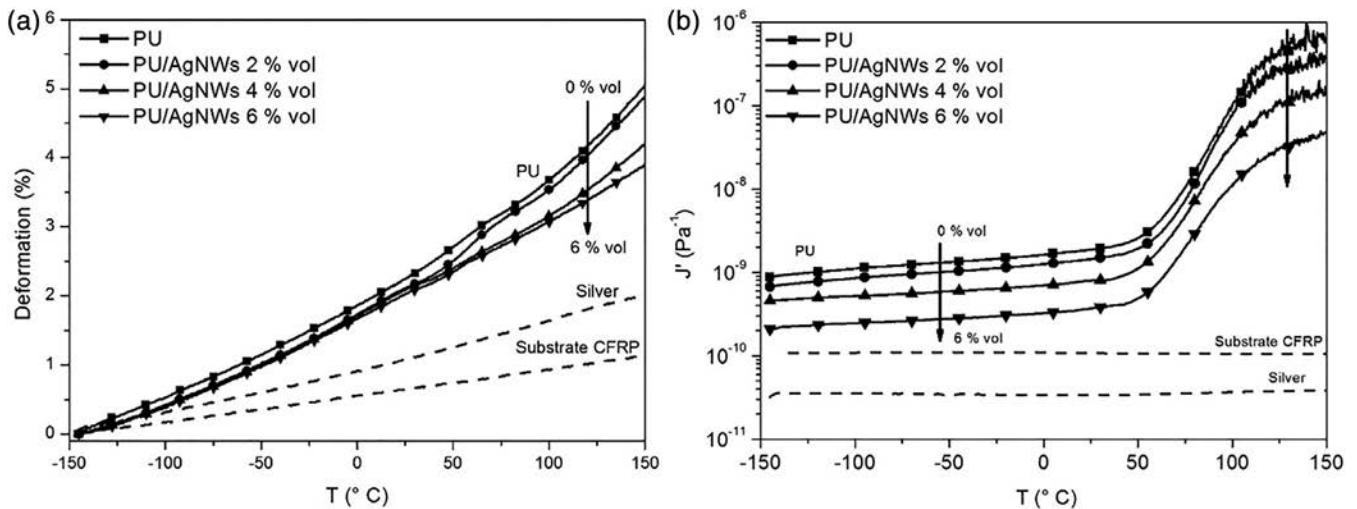
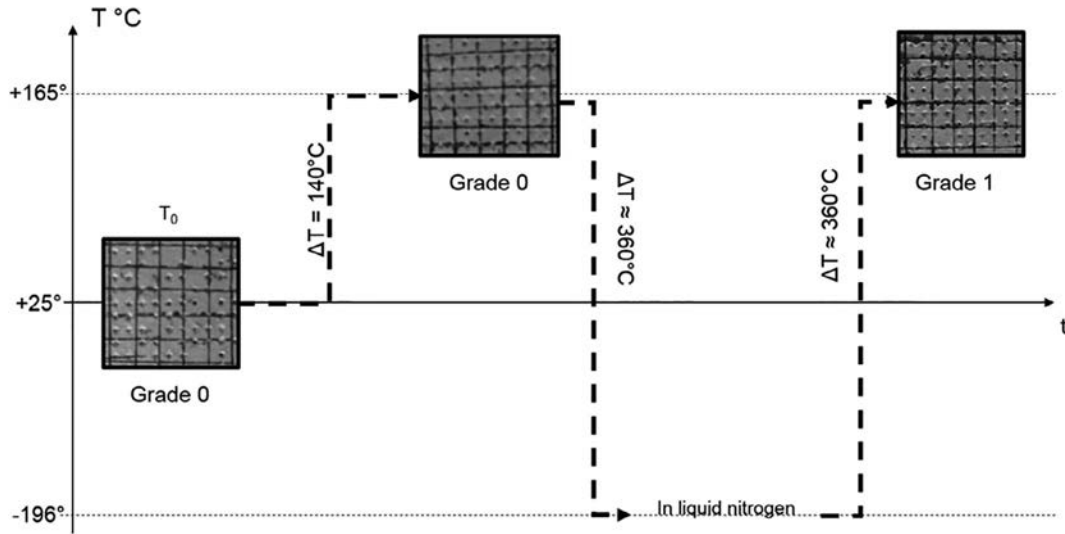


FIGURE 7 Strain and storage compliance of polyurethane (PU)/silver nanowires (AgNWs) coatings

**TABLE 3** Thermal expansion coefficients for the different configurations

$\alpha$ ( $10^{-6} \text{ K}^{-1}$ )	$T < T_g$	Silver	CFRP	PU/AgNWs (%vol)			
				0	2	4	6
	$T < T_g$	59	38	132	130	131	128
	$T > T_g$	59	38	285	280	211	169

Abbreviations: AgNWs, silver nanowires; CFRP, carbon fiber reinforced polymer; PU, polyurethane.



**FIGURE 8** Adhesion of the electrodeposition to the initial state and following two thermal shocks

### 3.4 | Electromagnetic shielding effectiveness

The shielding effectiveness tests are presented on the frequency range from 1 to 26 GHz. The shielding effectiveness and the 90 dB criterion expected by spatial industry are reported on Figure 9.

The CFRP substrate has the lowest attenuation and its shielding effectiveness decreases linearly with frequency range. This frequency behavior is well known in the literature for metallic grids.<sup>36</sup> The studied CFRP is constituted of twill weave carbon fiber; its shielding effectiveness was compared to a grid model illuminated by a plane wave:

$$SE = 20 \log \left( \frac{\lambda}{2g} \right) \quad (3)$$

With  $g$  the grid mesh and  $\lambda$  the wavelength.

For the grid model with for  $g = 20 \mu\text{m}$ , results are reported in dashed line on Figure 9. The CFRP frequency behavior could be compared to a  $20 \mu\text{m}$  grid. The equivalent spacing is the same order of magnitude than carbon fibers diameter near  $7 \mu\text{m}$ .

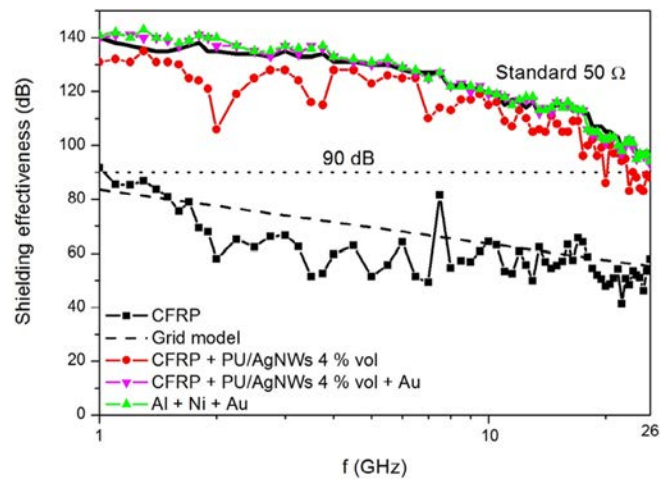


**FIGURE 9** Shielding effectiveness for studied configurations. AgNWs, silver nanowires; CFRP, carbon fiber reinforced polymer; PU, polyurethane [Color figure can be viewed at [wileyonlinelibrary.com](http://wileyonlinelibrary.com)]

The CFRP substrate coated with PU/AgNWs filled with 4%vol presents a shielding effectiveness higher than 90 dB up to 20 GHz. For specific frequency, as 2 GHz for example, we observe shielding effectiveness loss peak (for



neat CFRP also). It is a resonance effect; that is, for a given frequency, the transmitted wave in the casing is amplified and the shielding effectiveness decreases. The shielding effectiveness of a gold metallized aluminum cover (current solution) and the metallized CFRP substrate is shown on Figure 9. The two solutions have been electroplated by the same gold treatment. The gold layer thickness is about 3  $\mu\text{m}$ .

The aluminum cover is electroplated on two faces whereas the CFRP substrate on only one. The two solutions present a shielding effectiveness equivalent to 50  $\Omega$  standard (black line on the Figure 9) on all the frequency range. The AgNWs conductive coating concept allows the CFRP electrodeposition plating in the same classical conditions as metal substrate with equivalent shielding effectiveness.

## 4 | CONCLUSION

In space environment, the wide temperature range induces important thermal expansion. That is why CFRP metallization requires more attention. The classical metallization process based on direct metal deposition are not suitable. This work has demonstrated the crucial interest to use an intermediate polymer conductive coating. This layer allows us to realize an electrodeposition and its specific mechanical properties adapt the thermal expansion of the CFRP substrate.

The improved conductive film was achieved with a 4%vol AgNWs/PU coated by air spray process. For the electrodeposition, a limit current density has been determined near 0.1 A/dm<sup>2</sup>. The growth speed is 7  $\mu\text{m}/\text{h}$  at 0.1 A/dm<sup>2</sup> and the criterion of 5  $\mu\text{m}$  for the electromagnetic shielding is obtained after 45 min. The electromagnetic shielding tests shows that coated and electrodeposited CFRP is an acceptable solution up to 20 GHz. The shielding reaches an attenuation value higher than 90 dB between 1 and 26 GHz. Furthermore, this new process requires a soft surface preparation without chemical treatment and a solvent emission reduced by a waterborne PU coating. It is an original route to metallize various insulator substrate.

## ACKNOWLEDGMENTS

These results were obtained under the research project "SURFINNOV" at the IRT Saint Exupéry. We thank the industrial and academic members of the IRT who supported this project through their contributions, both financial and in terms of specific knowledge: (a) Industrial members: Airbus Defence & Space, Airbus Group Innovation, Airbus Helicopter, Airbus Operation, Akzo, GIT, Liebherr, Mapaero,

Mecaprotec, Prodem, Socomore, Stelia Aerospace, Thales Alenia Space. (b) Academic members: CIRIMAT, Laplace, UPS, and CNRS. We also thank the "Commissariat Général aux Investissements" and the "Agence Nationale de la Recherche" for their financial support in the "Programme d'Investissement d'Avenir" (PIA).

## ORCID

Antoine Lonjon  <https://orcid.org/0000-0002-4346-6543>

## REFERENCES

- [1] V. K. Hariharan, P. V. N. Murthy, A. Damodaran, N. D. Ghatpande, T. L. Danabalan, V. R. Katti. Satellite EMI/ESD Control Plan. *Electromagn. Interf. Compat. 10th Int. Conf. IEEE*. 501 507, 2008.
- [2] D. D. Chung, *Carbon* 2001, 39(2), 279.
- [3] Y. Yang, M. C. Gupta, K. L. Dudley, R. W. Lawrence, *Nano Lett.* 2005, 5(11), 2131.
- [4] N. Li, Y. Huang, F. du, X. He, X. Lin, H. Gao, Y. Ma, F. Li, Y. Chen, P. C. Eklund, *Nano Lett.* 2006, 6(6), 1141.
- [5] J. Liang, Y. Wang, Y. Huang, Y. Ma, Z. Li, J. Cai, C. Zhang, H. Gao, Y. Chen, *Carbon* 2009, 47, 922.
- [6] J. M. Thomassin, X. Lou, C. Pagnouille, A. Saib, L. Bednarz, I. Huynen, R. Jérôme, C. Detrembleur, *J. Phys. Chem. C* 2007, 111(30), 11186.
- [7] Z. Chen, C. Xu, C. Ma, W. Ren, H. M. Cheng, *Adv. Mater.* 2013, 25(9), 1296.
- [8] M. Bayat, H. Yang, F. K. Ko, D. Michelson, A. Mei, *Polymer* 2014, 55(3), 936.
- [9] Y. Gao, L. Huang, Z. J. Zheng, H. Li, M. Zhu, *Appl. Surf. Sci.* 2007, 253(24), 9470.
- [10] F. N. Cogswell, *Thermoplastic Aromatic Polymer Composites*, Butterworth Heinemann Ltd, Jordan Hill, Oxford 2013.
- [11] A. Brenner, G. Riddell, *J. Res. Natl. Bur. Stand.* 1947, 39, 385.
- [12] H. Schladitz, Metal deposition process. US2698812, 1955.
- [13] M. W. Croze, Method of coating polytetrafluoroethylene articles and resulting articles. US2689805, 1954.
- [14] G. Stremmsdoerfer, F. Ghanem, Y. Saikali, A. Fares Karam, *J. Mater. Sci.* 2003, 38(15), 3285.
- [15] W. S. Huang, M. Angelopoulos, J. R. White, J. M. Park, *Mol. Cryst. Liq. Cryst.* 1990, 189, 227.
- [16] A. V. Thakur, B. J. Lokhande, *Heliyon* 2019, 5, e02909.
- [17] M. Bazzaoui, J. I. Martins, E. A. Bazzaoui, A. Albourine, R. Wang, P. D. Hong, *Surf. Coat. Technol.* 2013, 224, 71.
- [18] D. K. Yfantis, S. I. Kakos, S. Lamprakopoulos, S. Depountis, C. D. Yfantis, Copper electrodeposition on insulators (plastics) using highly conductive polypyrrole films. Proc. 5th WSEAS Int. Conf. Environ. Ecosyst. Dev 190 194, 2006.
- [19] L. Q. Cortes, A. Lonjon, E. Dantras, C. Lacabanne, *J. Non Cryst. Solids* 2014, 391, 106.
- [20] D. Untereker, S. Lyu, J. Schley, G. Martinez, L. Lohstreter, *ACS Appl. Mater. Interfaces* 2009, 1(1), 97.
- [21] A. Lonjon, L. Laffont, P. Demont, E. Dantras, C. Lacabanne, *J. Phys. D Appl. Phys.* 2010, 43(34), 345401.
- [22] L. Ramachandran, A. Lonjon, P. Demont, E. Dantras, C. Lacabanne, *Mater. Res. Express* 2016, 3, 85027.

- [23] A. Lonjon, L. Laffont, P. Demont, E. Dantras, C. Lacabanne, *J. Phys. Chem. C* **2009**, *113*(28), 12002.
- [24] S. Wang, Y. Cheng, R. Wang, J. Sun, L. Gao, *ACS Appl. Mater. Interfaces* **2014**, *6*(9), 6481.
- [25] A. Lonjon, P. Demont, E. Dantras, C. Lacabanne, *J. Non Cryst. Solids* **2012**, *358*, 3074.
- [26] J. Audoit, L. Laffont, A. Lonjon, E. Dantras, C. Lacabanne, *Polymer* **2015**, *78*, 104.
- [27] V. Favier, R. Dendievel, G. Canova, *Acta Mater.* **1997**, *45*(4), 1557.
- [28] P. Ma et al., *ACS Appl. Mater. Interfaces* **2009**, *1*(5), 1090.
- [29] S. Barrau, P. Demont, A. Peigney, C. Laurent, C. Lacabanne, *Macromolecules* **2003**, *36*, 5187.
- [30] D. Carponcin, E. Dantras, G. Aridon, F. Levallois, L. Cadiergues, C. Lacabanne, *Compos. Sci. Technol.* **2012**, *72*, 515.
- [31] A. Lonjon, P. Demont, E. Dantras, C. Lacabanne, *J. Non Cryst. Solids* **2012**, *358*(2), 236.
- [32] D. Dupenne, A. Roggero, E. Dantras, A. Lonjon, T. Pierre, *J. Non Cryst. Solids* **2017**, *468*, 45.
- [33] Y. Sun, B. Gates, B. Mayers, Y. Xia, *Nano Lett.* **2002**, *2*, 165.
- [34] Y. Sun, Y. Yin, B. Mayers, *Chem. Mater.* **2002**, *14*(6), 4736.
- [35] F. Ghanem, Elaboration et caractérisation de films de cuivre par la méthode de dépôt chimique dynamique. Thèse de l'Ecole Centrale de Lyon, **2003**.
- [36] R. W. Evans, Design guidelines for shielding effectiveness, current carrying capability, and the enhancement of conductivity of composite materials. **1997**.

**How to cite this article:** Dupenne D, Lonjon A, Dantras E, Pierré T, Lubineau M, Lacabanne C. Carbon fiber reinforced polymer metallization via a conductive silver nanowires polyurethane coating for electromagnetic shielding. *J Appl Polym Sci.* 2020;e50146. <https://doi.org/10.1002/app.50146>